Palivizumab epitope–displaying virus-like particles protect rodents from RSV challenge

Jeanne H. Schickli,[1] David C. Whitacre,[2] Roderick S. Tang,[1] Jasmine Kaur,[1] Heather Lawlor,[1] Cory J. Peters,[2] Joyce E. Jones,[2] Darrell L. Peterson,[3] Michael P. McCarthy,[1] Gary Van Nest,[1] and David R. Milich[2]

[1]MedImmune, Gaithersburg, Maryland, USA. [2]VLP Biotech Inc., San Diego, California, USA. [3]Virginia Commonwealth University, Department of Biochemistry, Richmond, Virginia, USA.

Respiratory syncytial virus (RSV) is the most common cause of serious viral bronchiolitis in infants, young children, and the elderly. Currently, there is not an FDA-approved vaccine available for RSV, though the mAb palivizumab is licensed to reduce the incidence of RSV disease in premature or at-risk infants. The palivizumab epitope is a well-characterized, approximately 24-aa helix-loop-helix structure on the RSV fusion (F) protein (F254–277). Here, we genetically inserted this epitope and multiple site variants of this epitope within a versatile woodchuck hepadnavirus core–based virus-like particle (WHcAg-VLP) to generate hybrid VLPs that each bears 240 copies of the RSV epitope in a highly immunogenic arrayed format. A challenge of such an epitope-focused approach is that to be effective, the conformational F254–277 epitope must elicit antibodies that recognize the intact virus. A number of hybrid VLPs containing RSV F254–277 were recognized by palivizumab in vitro and elicited high-titer and protective neutralizing antibody in rodents. Together, the results from this proof-of-principle study suggest that the WHcAg-VLP technology may be an applicable approach to eliciting a response to other structural epitopes.

Introduction

Reverse vaccinology has accelerated the identification of new antigenic epitopes on infectious agents, tumors, and allergens, and has fueled the concept of epitope-focused vaccine design. However, the conversion of these antigenic epitopes into efficient immunogens deliverable as vaccines has remained a challenge. A number of epitope delivery or carrier platforms have been devised, but have been plagued by instability upon insertion of heterologous epitopes, the conformational requirements of nonlinear epitopes, and poor immunogenicity, protective efficacy, or yield. We used a combinatorial virus-like particle (VLP) technology and a model epitope from the respiratory syncytial virus (RSV) to address these obstacles.

RSV is a major cause of lower respiratory tract disease in infants and young children, and a vaccine to protect this susceptible population is a high priority (1–4). Development of an RSV vaccine has been hampered by the incidence of enhanced respiratory disease (ERD) following vaccination with formalin-inactivated RSV in the 1960s (5–7). Subsequent approaches have been to identify key neutralizing RSV proteins or epitopes to which a protective immune response can be safely generated, and development of modern pre- and postfusion RSV fusion (F) protein subunit vaccines is ongoing (8–10). Alternatively, an immunogen targeted to a single neutralizing epitope may provide protection as a stand-alone vaccine or serve to boost a specific protective immune response after priming with an RSV F vaccine.

In the late 1980s, a mouse mAb (no. 1129) directed to the F protein of RSV was found to have strong RSV-neutralizing capability over a broad range of RSV strains (11). mAb 1129 was subsequently humanized and named palivizumab. As administration of palivizumab is able to reduce the incidence of RSV disease, the epitope bound by palivizumab provides a well-characterized vaccine target likely to elicit a protective humoral immune response (12–14). Sequencing of palivizumab escape mutants identified aa 254–277 on the RSV F protein as the palivizumab-binding site (11, 15, 16). Although the palivizumab epitope (also referred to as antigenic site A or site II) is composed of contiguous aa in F, its helix-loop-helix secondary structure is critical for palivizumab binding (17–19). A number of groups have attempted to exploit the site A region to generate a focused immune response against RSV F, but in general, the polyclonal response to site A–based vaccines has been characterized by poor binding to intact RSV F protein, modest in vitro neutralization, and no evidence of protection from RSV challenge in vivo (20–22). Most recently, Correia and colleagues described a sophisticated approach that accurately reproduced the palivizumab epitope structure, but failed to produce a neutralizing Ab (nAb) response in rodents (23). Interestingly, 12 of 16 macaques produced RSV nAbs after 5 immunizations with these scaffolded immunogens, although no protection data were reported (23).

Our approach is to express the epitope on a highly immunogenic VLP. A VLP vaccine can capitalize on a regularly arrayed presentation of multiple copies of an epitope on each particle. The repetitive display of the epitope to antigen-presenting cells (APCs), including B cells, may serve to enhance the immune response (24–26). Ideally, VLPs self assemble to form uniform, thermodynamically stable particles. VLPs of human hepatitis

Authorship note: Jeanne H. Schickli and David C. Whitacre contributed equally to this work.

Conflict of interest: David R. Milich, David C. Whitacre, Cory J. Peters, and Joyce E. Jones are employees of VLP Biotech; Gary Van Nest, Michael P. McCarthy, Roderick S. Tang, Jeanne H. Schickli, Jasmine Kaur, and Heather Lawlor were employees of MedImmune when the work was performed. The research in this manuscript was funded by MedImmune.

Submitted: August 11, 2014; **Accepted:** January 22, 2015.

Reference information: *J Clin Invest*. 2015;125(4):1637–1647. doi:10.1172/JCI78450.

Table 1. Description of hybrid WHcAg VLPs

		Insertion in the VLP immunodominant loop		
Designation	VLP Carrier	Linker	Insert	Linker
VLP-19	Unmodified	GILE	NSELLSLINDMPITNDQKKLMSNN	L
VLP-59	Unmodified	–	NSELLSLINDMPITNDQKKLMSNN	–
VLP-74	Unmodified	GILA	NSELLSLINDMPITNDQKKLMSNN	L
VLP-75	Unmodified	GIL_	NSELLSLINDMPITNDQKKLMSNN	L
VLP-78	R-to-A motif	GILE	NSELLSLINDMPITNDQKKLMSNN	L
VLP-87	Truncated	GILE	NSELLSLINDMPITNDQKKLMSNN	L
VLP-88	N136P, A137P	GILE	NSELLSLINDMPITNDQKKLMSNN	L
VLP-90	Unmodified	GIL_	NSELLSLIHDMPITNDQKKLMSNN	L
VLP-93	C61S	GILE	NSELLSLINDMPITNDQKKLMSNN	L
VLP-97	Unmodified	–	NSELLSLINDMPITNDQKKLMSNN**V**	–
VLP-98	Unmodified	–	NSELLSLINDMPITNDQKKLMSNN**VQ**	–
VLP-99	Unmodified	–	NSELLSLINDMPITNDQKKLMSNN**VQI**	–

VLP carrier variants: (a) unmodified WHcAg; (b) C-terminal arginines mutated to alanines to abrogate ssRNA encapsidation by the VLP (R-to-A); (c) truncated on the C-terminus to abrogate ssRNA encapsidation (truncated); (d) mutated in a B cell epitope (N136P, A137P); or (e) mutated to eliminate a disulfide bond (C61S).

B virus core antigen (HBcAg) have been crystallized and are well characterized (27–30). VLPs composed of woodchuck hepadnavirus core (WHcAg) protein have essentially the same size and structure as those of HBcAg; however, derivation from a nonhuman pathogen provides advantages (31). Using a combinatorial approach, an epitope can be inserted into any one of 17 positions in immunodominant regions of the VLP. Combined with modifications to the epitope and/or the WHcAg, a library of hybrid VLPs can be generated, each displaying 240 copies of the inserted epitope on the surface (29, 31, 32).

We report herein that a proportion of hybrid VLPs were recognized by palivizumab and elicited RSV F-specific nAbs. In mice immunized with an exemplary WHcAg expressing the RSV F epitope aa 254–277 and challenged with WT RSV, viral titers were reduced by more than 99% compared with placebo.

Results

The WHcAg VLP displays RSV F aa 254–277. The palivizumab epitope or variants were cloned into the WHcAg gene for display in various positions, including the immunodominant loop region of the WHcAg-VLP (31, 32), to produce a series of constructs for screening (Figure 1 and Table 1). The large majority of designed hybrid VLPs assembled, bound palivizumab, and induced anti-F Abs in immunized mice. However, only a subset of hybrid VLPs elicited nAbs and also protected against an RSV challenge (Figure 1). We describe in detail VLP-19, a representative of the 6 VLP candidates that elicited the highest protective efficacy against RSV infection. VLP-19 contains RSV F254–277 inserted at residue 78 of the full-length WHcAg VLP and encapsidates ssRNA that acts as a TLR7 ligand (26).

Cryo-electron microscopic (cryo-EM) analysis was performed to characterize VLP-19 visually. At ×52,000 magnification, the particles carrying the insertions had a rougher surface appearance compared with the empty carrier WHcAg particles (Figure 2). Averaging performed by Nanoimaging Services revealed that the surface of VLP-19 was uniformly covered with spikes extending 2 to 4 nm from the surface of the spherical, approximately 29–nm diameter, particles. To determine whether the spikes indeed contained the 24-mer insert in the appropriate conformation, palivizumab Fabs were bound to the VLPs and EM analysis was again performed. The resulting images (Figure 2) are consistent with palivizumab Fabs binding to VLP surface spikes and demonstrate that the 24-mer encompassing aa 254–277 of the RSV F protein is successfully expressed on the surface of fully formed WHcAg VLPs.

SDS-PAGE and Western blot analysis were performed on VLP-19 and the carrier WHcAg and demonstrated that the monomer of VLP-19 contains an insert of the expected size (Figure 3A, lanes 1 and 2). Following transfer to a PVDF membrane, both VLP-19 and WHcAg were recognized by rabbit polyclonal antiserum against WHcAg (lanes 3 and 4), while only VLP-19 was recognized by palivizumab (lanes 5 and 6).

We further tested the ability of palivizumab to recognize VLP-19 in solid phase bound to an ELISA plate and in solution with a competitive ELISA assay. In the direct ELISA assay, we found that

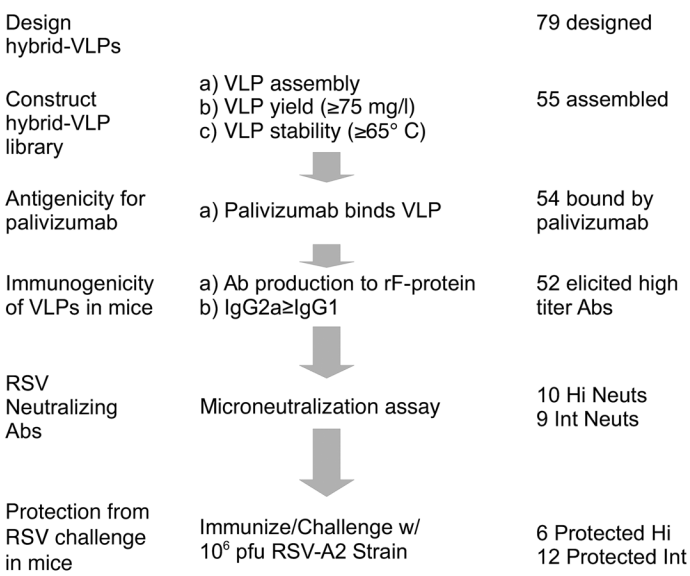

Figure 1. Downselection of hybrid WHcAg-VLPs displaying the RSV F254–277 palivizumab epitope. The hybrid VLPs were constructed with the following variations: (i) insertion of the epitope into the immunodominant loop between WHcAg aa 74 and 82 (31) either by engineered restriction sites (31) or fusion into the VLP ORF, (ii) fusion of the epitope to the N- or C-terminus of WHcAg, (iii) substituting the epitope for residues of WHcAg, (iv) insertion with flexible linkers flanking the epitope, (v) extension of the F254–277 epitope with native RSV F residues, and (vi) modifications in the WHcAg carrier (i.e., truncations, cysteine mutations, deletion of B cell epitopes). VLPs were expressed, purified, and screened according to the scheme depicted. For animal experiments, groups of 5 to 6 BALB/c mice were immunized as described in Methods. RSV-neutralizing titers (Neuts) were ranked as follows: high (Hi) ≥ 7; intermediate (Int) 5–7; low < 5 $\log_2$. Protection was ranked by $\log_{10}$ reduction in RSV lung titer as follows: high ≥ 2; intermediate 1–2; low < 1 $\log_{10}$ reduction.

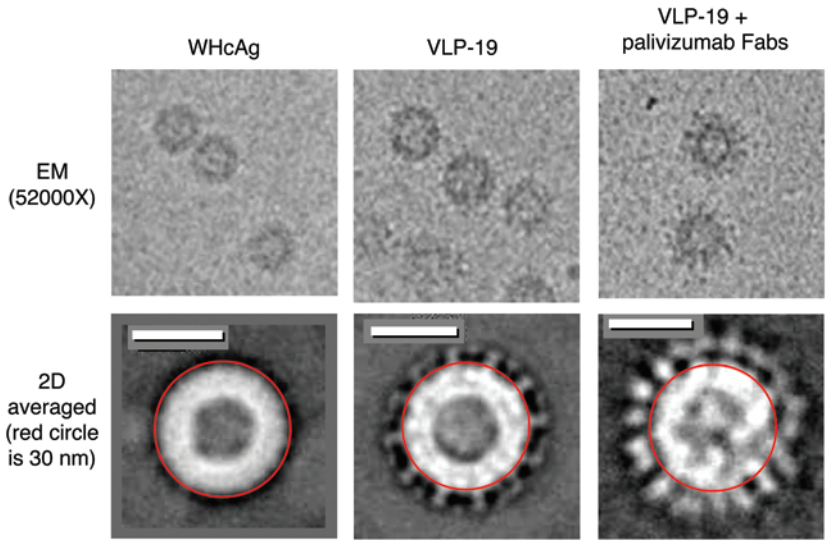

Figure 2. Electron micrographs of VLP. Cryo-EM analysis was performed on WHcAg, VLP-19, and VLP-19 plus palivizumab Fabs in PBS buffer. Samples were vitrified in liquid ethane and imaged with an FEI Tecnai T12 EM at NanoImaging Services. Scale bars: 20 nm.

palivizumab was able to bind VLP-19 (Figure 3B). As binding to a surface-bound antigen may be artifactual, we also tested the ability of VLP-19 to bind palivizumab in solution and thereby inhibit binding of the mAbs to soluble RSV F (sF) on the ELISA plate. These data show that palivizumab recognizes the fully formed VLP-19 in solution (Figure 3C).

To determine whether the RSV F aa 254–277 epitope displayed on VLP-19 is antigenically related to the epitope present during natural RSV infection, we tested human plasma for antibody specific for VLP-19 by ELISA. Due to multiple exposures to RSV, normal adult human plasma contains RSV-specific antibodies (2, 33). Human IgG in each of 42 adult plasma samples bound efficiently to VLP-19 and also to sF protein (Table 2 and Figure 3D). Therefore, VLP-19 could be used as a diagnostic to measure palivizumab-like antibody in naturally infected or vaccinated individuals. Taken together, these data indicate that the antigenicity of the palivizumab-specific RSV F254–277 epitope is maintained in the context of VLP-19.

VLP-19 elicits protection in rodents. BALB/c mice were immunized with two 40-μg doses of VLP-19 formulated with incomplete Freund's adjuvant (IFA). Negative and positive control groups received either PBS alone or 1 intranasal administration of live WT RSVA2, respectively (Figure 4). Two weeks after the second dose, sera were analyzed for F-specific IgG and for RSV neutralization, and then mice were challenged with 10^6 PFU WT RSVA2. Lung titers ($\log_{10}$ PFU/g) of mice 4 days after challenge were 3.9 ± 0.2 in the placebo group, and 1.1 ± 0.1 and 0.9 ± 0.1 for the WT RSV and VLP-19 groups, respectively (Figure 4A). The RSV microneutralization titers in sera on the day of challenge were 6.7 ± 0.4 and 7.7 ± 1.2 $\log_2$ for the WT RSV–infected and VLP-19–immunized mice, respectively, which are not statistically different ($P = 0.2$) (Figure 4B). The F-specific IgG titers were high for both groups, measuring 16.8 ± 0.8 and 17.6 ± 0.0 $\log_2$ for the WT RSV–infected and VLP-19–immunized groups, respectively (Figure 4C). Thus, immunization of mice with 2 doses of VLP-19 was able to elicit a 1000-fold reduction in lung titer and serum nAbs and RSV F-specific IgG titers, similar to mice following infection with WT RSV A2. Mice injected with VLP-19 in saline also produced nAbs that were antigen dose dependent and independent of adjuvant (Figure 5).

To determine whether protection in BALB/c mice was antibody mediated, pooled anti–VLP-19 sera (neutralization titer of 8.0 $\log_2$) were adoptively transferred to naive mice, which were subsequently challenged with WT RSV. 100 μl of anti–VLP-19 sera achieved a modest serum-neutralizing titer of 4.4 $\log_2$, compared with a neutralizing titer of 6.5 $\log_2$ in recipients of 1 mg/kg palivizumab. Nonetheless, lung viral titers were reduced 1.6 $\log_{10}$ in recipients of anti–VLP-19 sera and 3.4 $\log_{10}$ in palivizumab recipients (Figure 6).

Cotton rats, which are more permissive to RSV infection than mice, are a widely accepted model for studying RSV vaccines. Immunization with 3 doses of VLP-19 formulated in aluminum phosphate, an adjuvant approved for use in many vaccines, induced nAbs in 5 of 7 rats and protected 4 of 7 cotton rats from RSV challenge (Table 3). This indicates that a VLP carrying only the F254–277 epitope can elicit protection in cotton rats, although animal-to-animal variation was observed in protective efficacy and nAbs but not anti-F IgG production using alum as an adjuvant.

Anti–VLP-19 Abs are broadly neutralizing. An RSV plaque-reduction neutralization assay was performed with 2-fold dilutions of anti–VLP-19 mouse sera and palivizumab. For anti–VLP-19 sera, the RSV plaque reduction neutralization titer (PRNT) as measured by the IC_{50} was 7.2 $\log_2$, which is an approximately 1:150 dilution of sera (Figure 7A). For palivizumab, the PRNT as measured by the IC_{50} point was at a concentration of approximately 0.5 μg/ml. Thus, anti–VLP-19 sera provided the equivalent neutralizing capability of approximately 75 μg/ml palivizumab in this in vitro assay.

To investigate whether the anti–VLP-19 Abs and palivizumab were directed to the same epitope on RSV F, we performed a competitive ELISA on plates coated with sF. Dilutions of sera from VLP-19–immunized mice or a negative sera control were mixed with a constant concentration of palivizumab before addition to the sF-coated plates. Detection was for bound palivizumab. Anti–VLP-19 sera successfully competed with palivizumab for binding to sF (Figure 7B). The IC_{50} measurements of the binding curves for anti– VLP-19 sera were 10 $\log_2$ and 13 $\log_2$ for antisera taken after

Table 2. Recognition of RSV F protein and VLP-19 by human IgG

	ELISA endpoint titers ($\log_2$)	
Antigen	Young adult (20–30 years) $n = 19$	Elderly (65–85 years) $n = 23$
RSV F protein	12.8 ± 1.5	12.7 ± 2.2
VLP-19	11.4 ± 1.1	11.1 ± 1.4

The data are expressed as arithmetic mean value ± SD.

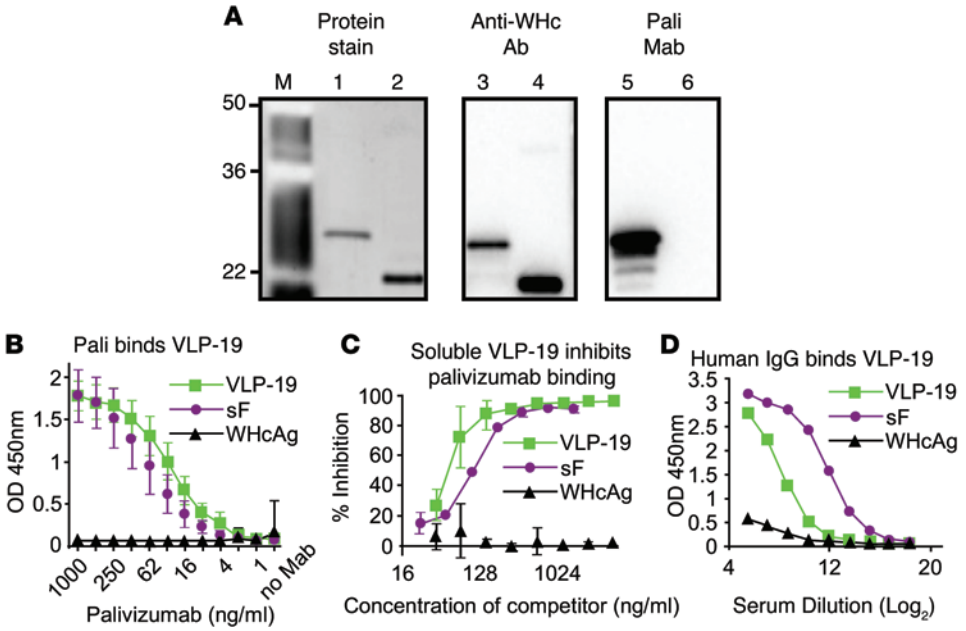

Figure 3. In vitro analysis of VLP-19 compared with WHcAg and sF. (**A**) VLP-19 (lanes 1, 3, and 5) and WHcAg (lanes 2, 4, and 6) VLPs were separated by SDS-PAGE. Total protein was visualized by SYPRO Ruby stain (lanes 1 and 2). Western blots were probed with anti-WHc Abs (lanes 3 and 4) or anti-RSV F palivizumab (lanes 5 and 6). (**B**) ELISA plates were coated with VLP-19, sF, or WHcAg. Coated plates were incubated with dilutions of palivizumab (Pali). Bound IgG was detected by HRP-conjugated anti-human IgG Abs. The ODs of 10 independently performed ELISA assays were averaged. Shown are the arithmetic mean averages of the ODs ± SD. (**C**) ELISA plates were coated with sF. Coated plates were incubated with dilutions of competitor (VLP-19, sF, or WHcAg) mixed with 100 ng/ml palivizumab. Bound IgG was detected by HRP-conjugated antihuman IgG Abs. The assay was performed 3 times, independently. The arithmetic mean averages of the percentage of inhibitions were calculated and plotted ± SD. (**D**) ELISA plates were coated with VLP-19, sF, or WHcAg. Coated plates were incubated with dilutions of human plasma, and bound IgG was detected by HRP-conjugated anti-human IgG Abs. For all ELISA assays, bound IgG was detected by HRP-conjugated anti-human IgG Abs. One representative ELISA assay is shown.

1 dose and 2 doses of VLP-19, respectively, suggesting an increase in titer of palivizumab-competing Abs following the boost.

The anti–VLP-19 sera were further evaluated and found to neutralize several RSV A and B clinical isolates as well as the palivizumab-resistant mutants (MARMs) S275F and S275L (Figure 8, A–E). However, anti–VLP-19 sera did not neutralize the K272Q or K272E MARMs (Figure 8F). These results illustrate the polyclonal nature of the anti–VLP-19 response and suggest differences in fine specificity compared with palivizumab.

Effect of epitope orientation. RSV F254–277 forms a helix-loop-helix motif, and McLellan and colleagues have described the contact points between the helices and motavizumab (an investigational drug derived from palivizumab) (17, 18). This work suggests that the relative orientation of the 2 helices is critical. If the α helices of the VLP-19 insert were constrained in a favorable presentation, we predicted that inserting aa between the insert and VLP would affect the antibody response to the insert. We incrementally extended the RSV F epitope by up to 3 residues at the C-terminus and tested the resulting VLP constructs for their ability to elicit a functional anti-RSV response (3 residues encompass roughly 1 revolution of an α helix). VLP-19 has linker regions that flank the 24-mer insert to accommodate the restriction sites used to clone the target sequence into the WHcAg gene, as described (32). For this experiment, the linker regions were first removed to juxtapose the α helices of the RSV F epitope more closely to those of the WHcAg. Next, the inserted RSV F epitope was extended by 1, 2, or 3 aa on the C-terminus. The resulting VLPs were tested for palivizumab binding in vitro and protection and immunogenicity in vivo (Table 4). Removal of the short linker regions yielded similar RSV sF-specific IgG titers (VLP-59 vs. VLP-19 in Table 4), but reduced the ability of palivizumab to detect the VLP and reduced protection and nAb titers. Addition of 1 residue to the C-terminus of the insert (VLP-97) augmented the ability of palivizumab to detect the VLP and improved protection compared with VLP-59 (Table 4). However, addition of 2 residues to the C-terminus of the insert (VLP-98) reduced the ability of the VLP to be detected by palivizumab and protection from challenge. Finally, addition of 3 residues (VLP-99) abolished the ability to elicit protection from challenge with WT RSV A2 (Table 4). Notably, the ability of palivizumab to detect VLP-99 in vitro was high, even though this VLP was not able to protect mice from challenge with WT RSV A2. For VLP-99, palivizumab binding may be able to induce an in vitro conformation that the motif does not attain in vivo. Taken together, these results suggest that the orientation of the α helices relative

Table 3. Immunogenicity/challenge study in cotton rats immunized with VLP-19 in alum

Immunogen	VLP-19							rRSV-F			PBS		
	no. 1	no. 2	no. 3	no. 4	no. 5	no. 6	no. 7	no. 1	no. 2	no. 3	no. 1	no. 2	no. 3
Anti–RSV-F (log_2)	15	15	16	17	15	15	16	18	19	19	0	0	0
Neut titer (log_2)	0	10	0	13	8	5	6	11	12	12	0	0	0
RSV lung titer (log_{10})	5	0.8	4.2	0.9	0.9	4.8	2.2	1	0.9	0.9	4.9	5	5.1

Limit of detection (LOD) for RSV-microneutralization titer and RSV lung titers was 3.3 log_2 and 0.8–1.0 log_{10}, respectively.

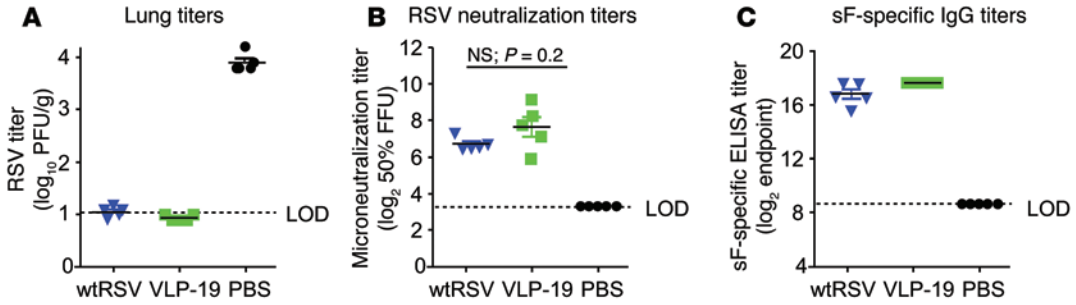

Figure 4. VLP-19 protects mice from challenge and elicits nAbs and F-specific IgG. BALB/c mice (n = 5) were intramuscularly dosed with 100 μl of either 40 μg VLP-19 formulated in IFA or PBS alone on days 0 and 14 or were infected with 10^6 PFU WT RSV A2 on day 0. On day 28, sera were sampled and mice were challenged with 10^6 PFU WT RSV A2. On day 32, lungs were harvested. (**A**) RSV in lung tissue was titered by plaque assay. (**B**) Heat-inactivated sera were tested for RSV microneutralization titers. (**C**) Sera were tested by ELISA for sF-specific IgG. This test was performed once with IFA (data shown) and 10 times with GLA-SE, which yielded similar results (data not shown). Data points for each animal are shown, with a black line through the arithmetic mean and colored error bars ± SEM. An unpaired 2-tailed Student's t test was performed to determine P values. $P > 0.05$ was considered not significant.

to each other in the helix-loop-helix motif is critical for the RSV F epitope to be displayed on the VLP in a manner that can elicit a -protective immune response.

Multiple VLPs elicit protection in mice. Five additional VLPs were examined in detail: VLPs 90 and 97 have modifications to the epitope; VLP-75 has a modification to the linker sequence; and VLPs 87 and 93 have changes in the WHcAg carrier (Table 1). Each variant may present the inserted epitope differently. Each VLP was tested in mice compared with sF and WT RSV controls, with sF and the VLPs formulated in glucopyranosyl lipid adjuvant (GLA-SE) and WT RSV administered as a live virus infection. Although it is difficult to compare such diverse immunogens, we utilized sF and WT RSV as positive controls to provide a reference to more traditional immunogens. The VLPs directed the immune response to only 24 aa from the virus, while sF and WT RSV elicited T and B cell responses to the entire extracellular domain of F and the full virus, respectively. The dose for each control was chosen based on prior experience to provide robust protection against RSV challenge. With these qualifications, the data for anti-F IgG titers, RSV microneutralization titers, and RSV lung titers are presented in Figure 9. VLPs 19 and 93 were analyzed in 1 experiment with the representative controls shown. Each of VLPs 75, 87, 90, and 97 was analyzed in separate experiments with data for their respective controls presented in Supplemental Tables 1–3 (supplemental material available online with this article; doi:10.1172/JCI78450DS1).

Immunization with the selected VLPs elicited IgG directed to RSV F, elicited nAbs, and protected mice from challenge with WT RSV A2 (Figure 9, A–D). The sF control elicited higher levels of anti-F IgG than each of the VLPs, as expected, due to the presence of a greater number of B cell epitopes on sF (11, 15, 16). In general, the WT RSV control elicited IgG levels that were similar to those for the VLPs, with differences being statistically different only for VLPs 87 and 97 (Figure 9A and Supplemental Table 1). Similar to the sF and WT RSV controls, all RSV-WHcAg VLPs elicited both TH1- and TH2-like anti-F Abs with the IgG2a subclass (TH1-like) predominant for all VLPs except VLP-87, which does not contain the TLR7 agonist (ssRNA) due to truncation of the WHcAg C-terminus (Figure 9B). The sF control appeared to elicit higher nAb titers in general; however, the differences were statistically significant only for the comparison with VLPs 75 and 90, while there were no significant differences between the nAb titers produced by infection with WT RSV and any of the VLPs (Figure 9C and Supplemental Table 2). VLPs 19, 75, 87, 90, and 93 each reduced RSV infection by 2 $\log_{10}$ PFU/g in 60% or more of the mice. VLP-97 demonstrated partial or complete protection in all mice (Figure 9D). Both the sF protein and WT RSV infection elicited reductions in RSV lung titers in a larger percentage of mice than the VLPs, but the reductions were statistically different only for VLP-97 (Figure 9D and Supplemental Table 3). VLP-90 was unique in that it provided good protection, but elicited lower nAb and IgG titers due to the N262H point muta-

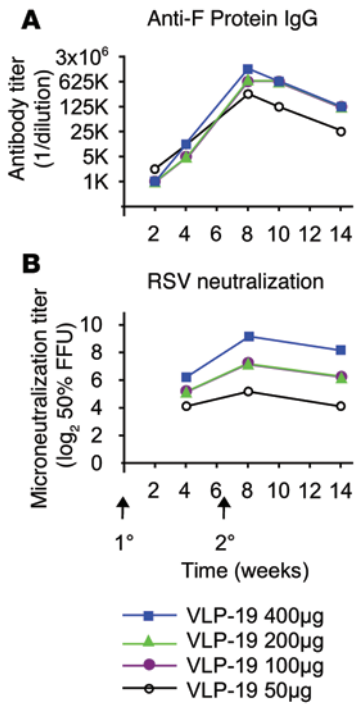

Figure 5. Immunogenicity of VLP-19 injected without adjuvant. Groups of 3 B10 × B10.S F1 mice were immunized i.p. with indicated doses of VLP-19 in PBS alone without adjuvant at weeks 0 and 6. Mice were bled, and serum was pooled. Serum was tested for (**A**) anti-RSV F IgG titers and (**B**) RSV microneutralization titers.

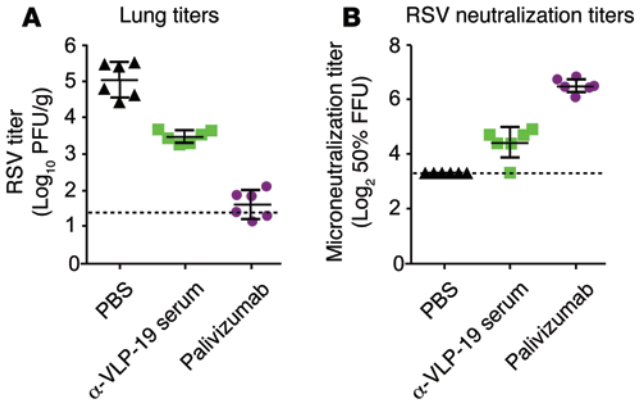

Figure 6. Passive transfer of anti–VLP-19 serum. Groups of 6 BALB/c mice were injected with 100 μl of pooled, anti–VLP-19 sera with a microneutralization titer of 8.0 $\log_2$ or 1.0 mg/kg of palivizumab or PBS administered 24 hours prior to challenge with 10^6 PFU WT RSV A2. (**A**) Protection of recipient mice was determined by titering RSV from lung tissue by plaque assay. (**B**) Heat-inactivated sera were tested for RSV microneutralization titers. Data points for each animal are shown. A black line is drawn through the arithmetic mean, and error bars indicate ± SEM.

tion in the F254–277 epitope. Presumably, this alteration in Ab fine specificity affects the in vitro microneutralization assay to a greater degree than potential in vivo antibody-mediated effector functions (i.e., antibody-dependent cellular cytotoxicity). If VLP-90 is excluded from the analysis, nAb titers of the 5 other VLPs correlate with protection ($P = 0.005$) and anti-F IgG titers show no statistical correlation with protection ($P = 0.26$).

Use of an adjuvant other than IFA revealed a dichotomy between production of anti-F IgG and RSV nAbs. Although 5 of 6 VLPs (VLPs 19, 75, 87, 93, and 97) consistently elicited high-titer anti-F IgG in all mice, the level of nAbs varied from mouse to mouse (Figure 9A compared with Figure 9C). This suggests that the ratio of anti-F IgG to nAbs is high in most anti-VLP sera and that functional nAbs represent a subset of the total anti-F response. In both the cotton rat and mouse studies, in which non-IFA adjuvants were used, some cohorts contained well-protected, partially protected, and a minority of unprotected animals. The observed animal-to-animal variation cannot be attributed to lack of T cell helper function because the anti-WHc (not shown) and anti-F IgG responses were consistently high, indicating efficient T cell help provided by WHcAg-specific T cells. Because B cell Ig receptor rearrangement is a stochastic process, even in inbred rodents, lack of a response to a single B cell specificity may represent a functional "hole" or at least a "leak" in the B cell repertoire.

Fine specificity of Ab responses can vary. To assess differences in Ab fine specificity, antisera to the hybrid VLPs were tested by ELISA against a panel of 60 F254–277 peptide analogs (i.e., truncations, single/multiple mutations). All anti-VLP sera recognized sF, but the fine specificity patterns against 10 representative peptides were strikingly different for each VLP antisera (Figure 10). Whereas palivizumab defines a single epitope within the F254–277 sequence, the Ab responses to the hybrid VLPs are polyclonal, potentially representing a number of site A specificities, including those competitive with palivizumab. Moreover, the fine specificities can be unique to each hybrid VLP.

To test the possibility that differing F254–277–specific neutralizing B cell specificities may be induced by the various VLPs, 4 individual mice that failed to produce nAbs after 2 doses of VLP 74, 78, 87, or 88 (which elicited nAbs in some but not all mice) were given a single heterologous boost with VLP-19. All 4 of the mice seroconverted to nAb positivity after the heterologous boost, suggesting that the "hole" in the B cell repertoire for certain VLPs does not necessarily extend to other VLPs (Table 5).

Discussion

The purpose of this study was 2-fold: first, to present the palivizumab-specific, conformationally dependent F254–277 epitope on the WHcAg VLP platform in a manner that maintained its secondary structure and antigenicity; and second, to demonstrate that hybrid VLPs expressing this single RSV F epitope could generate nAbs able to protect against RSV challenge. These goals were achieved by producing a library of 55 self-assembling, stable, hybrid VLPs in high yields and selecting for palivizumab binding (54 of 55), ability to induce RSV F-binding IgG (52 of 55), ability to induce RSV

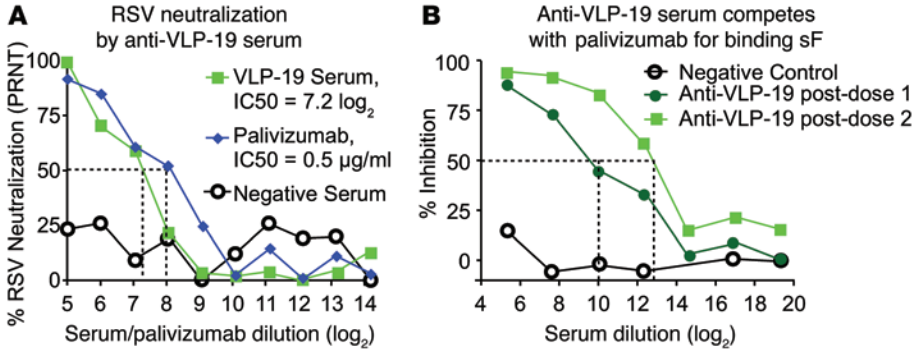

Figure 7. Murine anti–VLP-19 sera neutralize RSV and competes with palivizumab. (**A**) PRNT RSV neutralization assay was performed with heat-inactivated sera from VLP-19–immunized mice and palivizumab. (**B**) ELISA plates were coated with sF and incubated with a constant amount of palivizumab mixed with dilutions of either negative sera or anti–VLP-19 sera. Bound palivizumab was detected with HRP-conjugated anti-human Abs. Following washes, color was developed with tetramethylbenzidine followed by 0.1 N HCl. OD was read at 450 nm, and percentage of inhibition was calculated by comparison with a negative control. Data shown reflect 1 of 3 independently performed experiments.

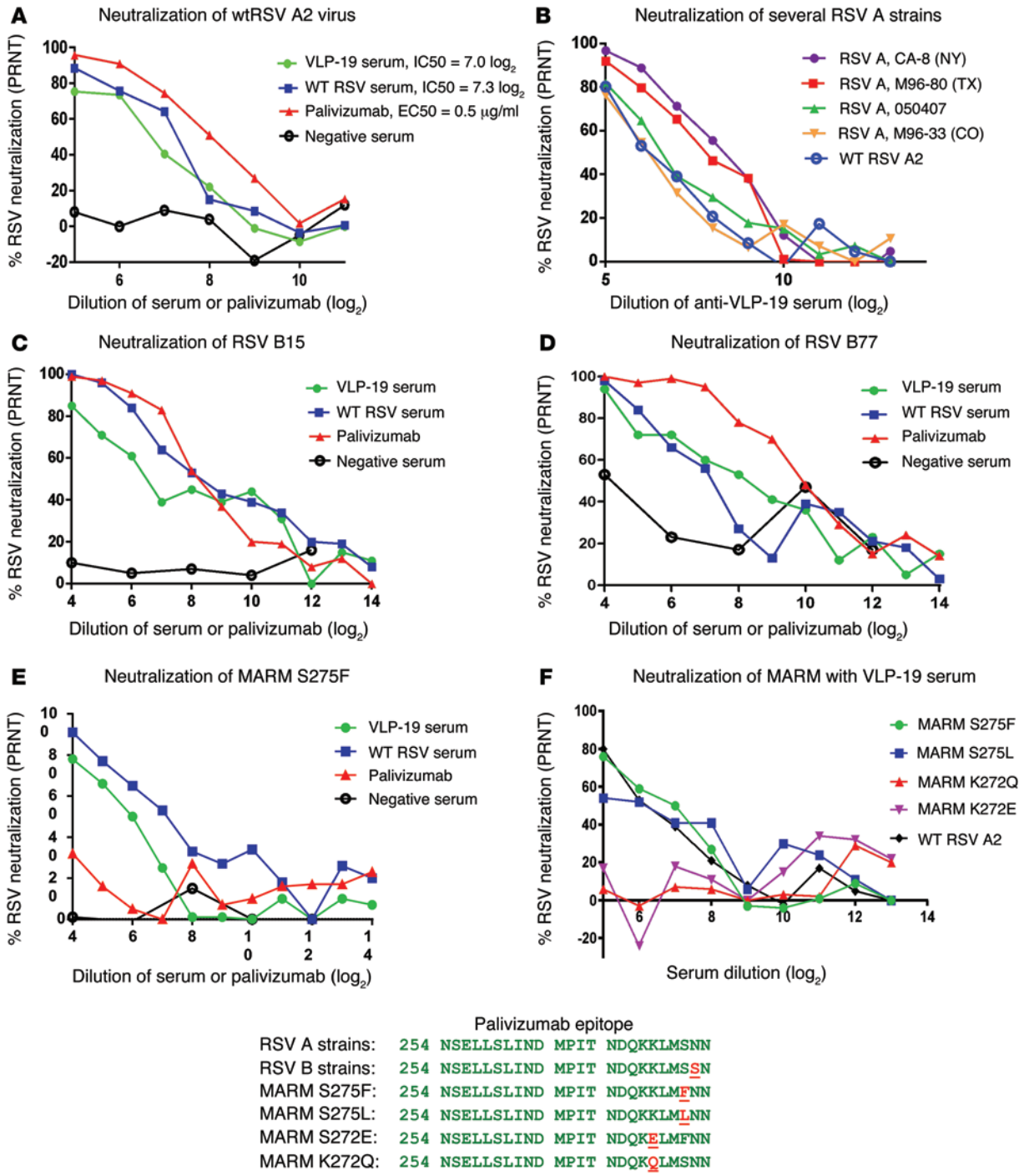

Figure 8. Anti–VLP-19 serum neutralization of RSV-A and RSV-B strains and MARMs. Dilutions of heat-inactivated serum or palivizumab were mixed with 100 to 200 PFU of RSV virus and incubated 1 hour; titers were measured by plaque assay. Anti–VLP-19 serum-neutralized WT RSV A2 (**A**), several recent RSV A clinical isolates (**B**), 2 RSV B clinical isolates (**C** and **D**), and palivizumab antibody escape mutant (MARMs) with a mutation at aa 275 (**E** and **F**). Anti–VLP-19 serum did not neutralize MARMS with a mutation at aa 272 (**F**). Sequences of the RSV F protein site A are shown.

nAbs (19 of 55), and ability to elicit protection against an RSV challenge (18 of 55). To our knowledge, this is the first demonstration of potent neutralization and protection from RSV challenge provided by recombinant, epitope-focused immunogens displaying only the RSV F254–277 epitope. This achievement also extends the application of the WHcAg hybrid VLP technology to the presentation of other epitopes requiring a specific conformation.

The WHcAg VLP may be uniquely suited as a platform for the RSV F254–277 epitope. The immunodominant spikes on the WHcAg are structurally similar to the F254–277 epitope in that both have a helix-loop-helix structure. The combinatorial technology developed for the WHcAg platform permits an empirical approach to reproducing the secondary structure of the F254–277 epitope on the hybrid VLPs (32). Although the precise etiology of

Table 4. In vitro and in vivo data for modified VLPs

Immunogen	Insert	Modification	Palivizumab binding in vitro (sF = 100%)	RSV lung titer after challenge (log_{10} ± SD PFU/g)	RSV neut titer (log_2 ± SD)	sF-specific IgG titer (log_2 ± SD)
Placebo	NA	NA	NA	3.9 ± 0.2	LOD[A]	LOD[B]
VLP-19	254-277	Linkers included	100%	0.9 ± 0.1	7.7 ± 1.2	17.2 ± 0.5
VLP-59	254-277	Linkers removed	83%	2.0 ± 1.0	5.2 ± 3.4	17.0 ± 0.9
VLP-97	254-278	Linkers removed (+1)	112%	1.1 ± 0.1	6.9 ± 2.8	17.2 ± 0.5
VLP-98	254-279	Linkers removed (+2)	47%	2.8 ± 1.0	3.9 ± 1.4	13.4 ± 1.6
VLP-99	254-280	Linkers removed (+3)	95%	3.8 ± 0.3	LOD*	16.4 ± 0.4

[A]LOD = 3.3 log_2. [B]LOD = 8.6 log_2. This experiment was performed once with IFA (data shown) and once with a proprietary adjuvant that yielded similar results (data not shown).

ERD caused by vaccination with formalin-inactivated RSV is not known, studies have identified several immunological markers less likely to be associated with ERD. For example, several studies have suggested that a TH2 bias correlates with ERD in rodent models and a TH1 bias may contribute to a protective immune response (34, 35). WHcAg VLPs elicit TH1-biased antibody isotypes that are enhanced by the encapsidated ssRNA that acts as a TLR7 agonist (26, 36). Nonneutralizing Abs may be implicated in ERD. Targeting a single neutralizing epitope avoids production of nonneutralizing Abs directed to non–site A epitopes of RSV F; however, site A-containing VLPs can also elicit nonneutralizing Abs, albeit restricted to site A. In addition, WHcAg VLPs displaying the palivizumab epitope will not prime F protein–specific T cells, which have been implicated in ERD (34).

Generation of multiple protective hybrid VLPs illustrates the power of the WHcAg combinatorial technology and allowed us to ask the question, are there biological consequences to the targeting of a single B cell epitope in vaccine design? In some instances,

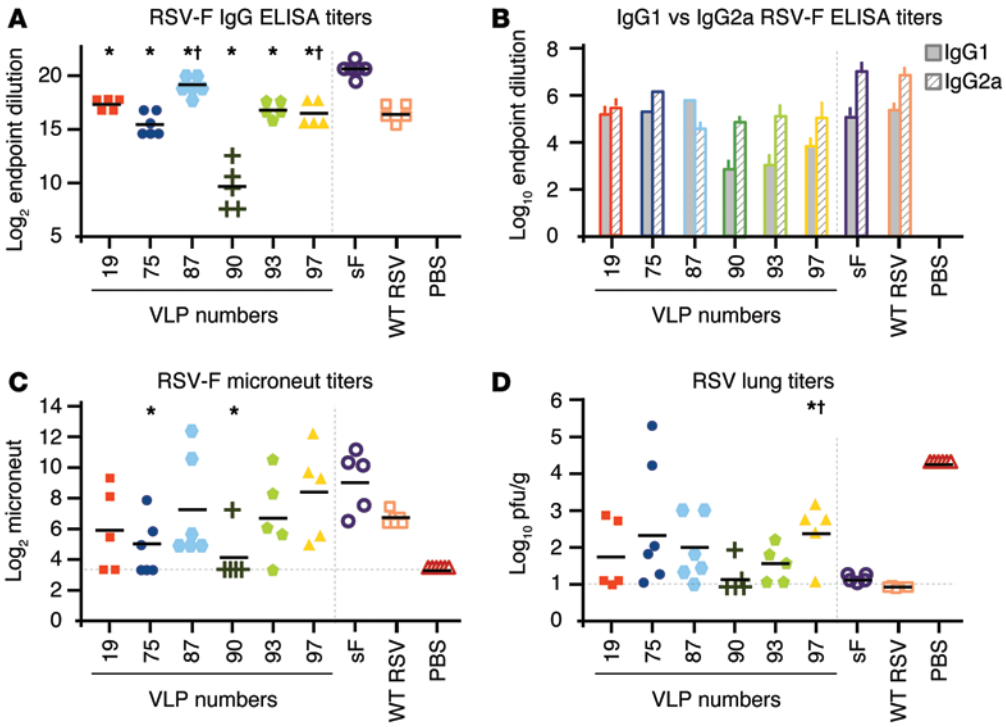

Figure 9. Immunogenicity and protective efficacy of RSV-WHc VLPs. Groups of 5 to 6 BALB/c mice were immunized and boosted with the indicated hybrid VLPs, sF (positive control), infected with WT RSV (positive control), or injected with PBS (negative control). (**A** and **B**) Anti-F IgG titers and IgG1/IgG2a isotype titers were determined by ELISA, respectively. (**C**) RSV microneutralization titers were determined. (**D**) Two weeks after the final bleed, mice were challenged with 10^6 PFU of WT RSV A2 and lung virus load determined by plaque assay. Mice were immunized with 40 μg RSV-WHcAg VLPs or 0.5 μg sF in GLA-SE. Because the F254–277 insert represents approximately 10% by weight of the VLPs, the functional dose of the F254–277 epitope within each VLP was approximately 4 μg. Comparison with the concurrent sF or WT RSV control groups was determined by 2-tailed Student's *t* test (homoscedastic) for anti-F IgG titers in **A**, RSV-microneutralization titers in **C**, and protection in **D**. **P* < 0.05, from sF. †*P* < 0.05 from WT RSV control (full data in Supplemental Tables 1–3). The sF, WT RSV, and PBS groups are representative of multiple experiments. Supplemental Tables 1–3 present the statistically relevant comparisons, which are most notable for VLP-97 in **A**. Excluding VLP-90 from the statistical analysis as discussed in the text, RSV microneutralization titers for the other VLPs correlate with protection ($r = -0.48$, $n = 27$, $t = 2.73$, and $P = 0.005$). In contrast, RSV F IgG ELISA titers show no statistical correlation with protection ($r = -0.13$, $n = 27$, $t = 0.656$, and $P = 0.26$). A 1-tailed analysis was used. $P \leq 0.05$ is considered statistically significant.

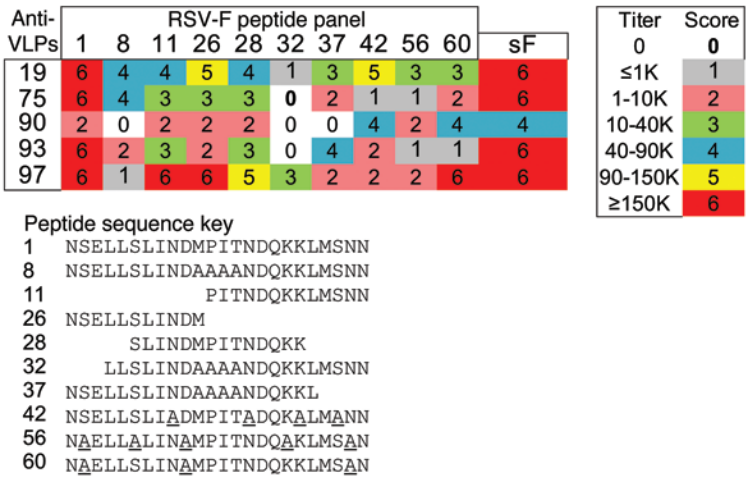

Figure 10. Variability in fine specificity of Ab responses. Antisera directed to VLPs 19, 75, 90, 93, or 97 were tested by ELISA for binding to sF or a panel of F254–277 peptide analogs. Plates were coated with the peptides diluted to 10 μg/ml or sF diluted to 0.2 μg/ml. A score of 0 to 6 was assigned, based on the endpoint dilution titer, as indicated. Sequences for each peptide are provided.

we observed animal-to-animal variation that was apparent in the nAb response but not in anti-F IgG production. Due to the stochastic nature of B cell Ig receptor rearrangement and because nAbs represent a limiting subset of the total anti–F254–277 response, this animal-to-animal variation may be due to functional "holes" in the B cell repertoire. A hole in the B cell repertoire has been shown to explain a compromised nAb response directed to a single epitope on a viral protein (37). This phenomenon may be especially relevant for epitope-focused vaccines due to the limited B cell epitope or epitopes targeted. In this context, species-to-species variation was observed in a study by Correia and colleagues in which immunization with an epitope-focused RSV-F vaccine produced no nAbs and only limited F-binding Abs in mice, yet nAbs were elicited in macaques (23). However, even in the macaques, nAbs were produced in only 7 of 16 animals after 3 immunizations and in 12 of 16 animals after 5 immunizations (23).

In our experience, holes or leaks in the B cell repertoire can be ameliorated by increasing the immunogen dose or potency of the adjuvant used, most likely due to the recruitment of low-frequency and/or low-affinity B cells by these measures. One method to mitigate animal-to-animal variation may be to include other highly neutralizing epitopes. A recent study identified an RSV F epitope targeted by the highly neutralizing D25 mAbs (38). While the palivizumab epitope is present on both pre- and postfusion F, the D25 epitope is present exclusively on prefusion F and represents another candidate to be considered for inclusion in an epitope-focused RSV vaccine. However, adding additional heterologous epitopes may not always be possible or desirable. Another method to mitigate variation is to include multiple iterations of the same or a similar epitope, as exemplified herein by VLPs 19, 75, 90, 93, and 97. These hybrid VLPs individually elicited protective nAbs, however, with different fine specificities. Therefore, mixing hybrid VLPs would enhance "intra–site A" B cell diversity and lessen the risks of nonresponse at the B cell level.

A goal of an epitope-focused approach, as described in the current study, is to determine the lower limits of antigenic diversity capable of eliciting a protective immune response. Herein, we demonstrate that a single 24-aa conformational domain (the palivizumab epitope) in the F protein presented on the WHcAg VLP carrier is sufficient to elicit substantial protection in animal models. As a practical matter, WHcAg VLPs are inexpensive to produce, being fully recombinant, highly thermostable (not requiring a cold chain), and expressed in bacteria, making the technology practical for use outside the first world. Thus, a WHcAg/RSV F hybrid VLP approach offers the potential for development as a component of or as a stand-alone RSV vaccine.

Table 5. A single VLP-19 boost rescues nAb nonproducers

	Neutralization titers (log_2)	
VLP	After 2 immunizations	After VLP-19 boost
VLP-74	0	3.3
VLP-78	0	4.9
VLP-87	0	5.1
VLP-88	0	5.1

Methods

Construction and expression of recombinant hybrid WHcAg particles. Full-length WHcAg (aa 1 to 188; GenBank NC_004107) was expressed from the pUC-WHcAg vector under the control of the Lac operon promoter, as described previously (31, 32). RSV F epitope sequences were designed to contain unique enzyme restriction sites at both the 5′ and 3′ ends to facilitate insertion into the pUC-WHcAg vector. For VLP-19, short linker regions encoding Gly-Ile-Leu on the N-terminus and Leu on the C-terminus were added to the heterologous insert as previously described (31). VLP-59 and VLPs 97 to 99 did not contain the short linker regions. Plasmids were transformed into chemically competent TOP10 *E. coli* (Invitrogen) according to the manufacturer's protocol. Proteins were expressed from the TOP10 strain and purified through hydroxyapatite followed by gel filtration chromatography on a Sepharose 4B (Pharmacia) column as described previously (31). The size and antigenicity of each hybrid WHc/RSV F protein was confirmed by SDS-PAGE and Western blotting. Yields generally exceeded 75 mg/l.

SDS-PAGE and Western blotting. 1 μg of material was separated in a 12% SDS-PAGE Tris-glycine gel that was stained with SYPRO Ruby (Invitrogen). Duplicate gels were transferred to PVDF membranes (Invitrogen) and probed with either palivizumab (MedImmune) followed by HRP-conjugated anti-human Abs (Dako) or with anti-WHc rabbit Abs (in house) followed by HRP-conjugated anti-rabbit Abs (Dako). Signal was developed with electrochemiluminescence solution (Thermo Scientific). Bands were visualized on a GE ImageQuant LAS 4000 analyzer.

EM. At NanoImaging Services, cryo-EM analysis was performed on WHcAg, VLP-19, and VLP-19 with palivizumab Fabs in PBS buffer. Palivizumab Fabs were generated with an Immunopure Fab kit (Thermo Scientific). 20 μl of VLP-19 at 1.0 mg/ml was mixed with 20 μl of Fabs at 1.0 mg/ml in PBS buffer and incubated for 4 hours at room

temperature (RT) prior to EM analysis. Briefly, a 3 μl drop of sample buffer was applied to a holey carbon film on a 400-mesh copper grid and vitrified in liquid ethane. The grids were stored under liquid nitrogen prior to imaging with an FEI Tecnai T12 EM, operating at 120 keV equipped with an FEI Eagle 4k × 4k CCD camera at less than 170.

ELISA assay. High-binding ELISA plates (Costar) were coated overnight with 0.2 μg/ml of test VLP, VLP-19, sF as positive control, or WHcAg as negative control in PBS. Plates were blocked with SuperBlock (Thermo Scientific). Two-fold dilutions of palivizumab at 1 mg/ml or human plasma samples were diluted in SuperBlock, and 50 μl per well was applied to the plates for 1 hour. After 4 washes in 0.5% Tween 20 in PBS buffer, HRP-conjugated anti-human Abs diluted to 1:5000 in superblock were applied for 1 hour. After washing, color was developed with 100 μl/well tetramethylbenzidine (Sigma-Aldrich). The reaction was stopped by addition of 100 μl per well 0.1 N HCl, and OD at 450 nm was read on an ELISA plate reader. The OD for sF-coated wells was between 1.5 and 2.5.

For competition ELISA assay with VLPs, as in Figure 3C, a constant concentration of 100 ng/ml palivizumab was mixed with 2-fold dilutions of VLP-19, WHcAg carrier, or sF; and the mixture was applied to the ELISA wells. Detection was performed with HRP-conjugated anti-human Abs to detect bound palivizumab. Data were plotted as percentage of inhibition. For mouse serum ELISA assays, as in Figure 4C, 2-fold dilutions of mouse serum were prepared in 3% BSA in PBS. The endpoint titer was calculated as the highest dilution with an OD greater than or equal to 2× blank. For competition ELISA with anti–VLP-19 serum, as in Figure 7B, 2-fold dilutions of anti–VLP-19 or control serum were mixed with 10 ng/ml palivizumab and applied to sF-coated ELISA plates. Detection was performed with HRP-conjugated anti-human antibody. For calculating percentage of binding, as in Table 4, VLP-coated and sF-coated wells to which 0.5 μg/ml palivizumab had been applied were compared. The OD for sF-coated wells was set at 100%, and the ODs for the VLP-coated wells were calculated relative to that 100% mark.

Mouse immunization and challenge. For initial screening of VLPs, groups of 5 to 6 BALB/c mice were immunized with hybrid VLPs: 20 or 40 μg emulsified in IFA (Sigma-Aldrich); 100 μg absorbed to alum (250 μg Adjuphos [Brenntag Biosector] or alum hydroxide gel [Sigma-Aldrich]), 40 μg mixed with GLA-SE (39) (Immune Design Corp.), or 50 to 400 μg injected in sterile PBS. For efficacy testing, female BALB/c mice, 6 to 8 weeks of age, were randomly divided into cohorts of 5 and consecutively numbered in the animal care facility at MedImmune according to IACUC procedures. On days 0 and 14, mice ($n = 5$) were immunized intramuscularly with 40 μg of the VLP to be tested or PBS (50 μl total volume) mixed with 50 μl IFA (Imject from Pierce) or 100 μg of VLP plus 250 μg AdjuPhos (Brenntag Biosector) or 40 μg of VLP (50 μl total volume) mixed with 50 μl of GLA-SE (39) (Immune Design Corp.) or 50 to 400 μg of VLP in 100 μl saline. RSV sF protein as described in Cherukuri et al. (8) was used as a positive control, and mice were injected with 0.5 μg in the various adjuvants. A final cohort of mice received 1 dose of 10^6 PFU WT RSV A2 (100 μl total volume) intranasally on day 0. For RSV challenge experiments, on day 28, sera were collected and mice were challenged with 10^6 PFU of WT RSVA2 (100 μl total volume) delivered intranasally. Four days after challenge, lung tissue was harvested, kept on ice, weighed, and homogenized in 2 ml Opti-MEM within 3 hours of harvest. Following a low-speed spin at 220 *g* for 5 minutes, the lung supernatants were titered by plaque assay. For heterologous VLP boosting depicted in Table 5, mice were selected that did not produce nAbs after 2 doses (20 and 10 μg) in IFA of the indicated VLPs (i.e., 74, 78, 87, or 88). These nAb-nonproducing mice were boosted with a single dose of VLP-19 (20 μg in IFA). Neutralizing titers were determined 3 weeks after the VLP-19 boost.

Five mice were used because, with a normal distribution and expected SD of 0.5 or less, 5 data points were expected to be sufficient to discern whether VLP-19 provided protection by reducing RSV lung titers by 2 or more $\log_{10}$ compared with placebo titers of approximately 4 $\log_{10}$ PFU/g.

Rat immunization and challenge. Cotton rats were immunized at 6-week intervals with 3 doses of VLP-19 in alum (100 μg + 250 μg alum), rRSV-F protein (0.5 μg + 250 μg alum), or PBS. Two weeks after the final dose, rats were bled and challenged with 10^6 PFU of WT RSVA2. Serum anti-F Abs were measured by ELISA, and RSV neutralization titers were determined by microneutralization assay. Four days after challenge, lungs were harvested to measure RSV titer by plaque assay.

Plaque assay. Ten-fold dilutions of virus in lung samples were made in Opti-MEM. 10^{-1}, 10^{-2}, and 10^{-3} dilutions of virus were applied to monolayers of Vero cells in TC6-well tissue culture plates. Vero cells were purchased from ATCC and tested for mycoplasma in the MedImmune cell culture facility. After 1 hour, the inoculum was replaced with methylcellulose-supplemented medium (2% methylcellulose mixed 1:1 with 2× L-15/EMEM [SAFC] supplemented with 2% FBS, 4 mM L-glutamine, and 200 U penicillin with 200 μg/ml streptomycin [Gibco; Life Technologies]) and incubated at 35°C for 4 to 5 days. Overlay was aspirated, and cells were immunostained with goat RSV Abs (Chemicon 1128) followed by HRP-conjugated anti-goat Abs (Dako). Red-colored plaques were developed with 3-amino-9-ethylcarbazole (Dako). Titer was recorded as PFU/g lung tissue. Consecutive sample numbers were titered consecutively. Analysts who performed the plaque assay may have been aware of the correspondence between the animal number and the assigned cohort.

RSV plaque reduction neutralization assay. Serum was heat inactivated at 56°C for 50 minutes. Dilutions of serum were combined with 100 or 200 PFU of RSV in Opti-MEM and incubated at 35°C for 1 hour before applying to 80% confluent monolayers of Vero cells in TC6-well plates. Cells were incubated with the serum-virus mixture for 1 hour. The inoculum was aspirated, and cells were overlaid with methylcellulose-supplemented medium, incubated for 5 days, and immunostained as for plaque assay as described above. The PRNT was calculated as the dilution at which 50% of RSV plaques were neutralized compared with controls with no serum.

RSV microneutralization assay. Serum was heat inactivated at 56°C for 50 minutes. Dilutions of serum were combined with 500 PFU of GFP-expressing RSV (RSV/GFP) and incubated at 33°C for 1 hour before applying to monolayers of Vero cells in 96-well plates in triplicate. After incubation for 22 hours, fluorescent foci units (FFU) were enumerated by an Isocyte imager. The reported neutralization titer is the interpolated dilution at which 50% of the input RSV/GFP virus was neutralized. Consecutive sample numbers were titered consecutively. Analysts who performed the RSV microneutralization assay were blinded with respect to the animal number and cohort.

Statistics. Prism Graphpad software was used to calculate the arithmetic mean and SEM for each group of animals used for Figures 4, 6, and 9, and the 2-tailed Student's *t* test was used for Figure 4. Microsoft Excel software was used to calculate the arithmetic mean and SD for data points in Figure 3 and Tables 2 and 4 and the correlation coeffi-

cients (r) between RSV lung titers and RSV microneutralization and IgG titers for Figure 9. The statistical formula used for the critical t value was $t = r \times \text{sqrt}((n-2)/(1-r^2))$. A standard statistics table was used to determine the P value for a 1-tailed analysis for each correlation and t value. $P < 0.05$ was considered significant and $P > 0.05$ statistically insignificant.

Study approval. Animal handling and procedures were conducted according to animal protocols approved by the review committees at MedImmune and the facility used by VLP Biotech to house animals (Explora Biolabs).

Acknowledgments

We acknowledge the contributions of the scientists in the analytical research department at MedImmune who performed the RSV microneutralization assays and the personnel in the animal care facility for their technical expertise.

Address correspondence to: David R. Milich, Janssen Labs: VLP Biotech Inc., 3210 Merryfield Row, San Diego, California 92121, USA. Phone: 858.242.1524; E-mail: dmilich@vlp-biotech.com.

1. Collins PL, Graham BS. Viral and host factors in human respiratory syncytial virus pathogenesis. *J Virol*. 2008;82(5):2040–2055.
2. Hall CB. The burgeoning burden of respiratory syncytial virus among children. *Infect Disord Drug Targets*. 2012;12(2):92–97.
3. Hall CB, et al. The burden of respiratory syncytial virus infection in young children. *N Engl J Med*. 2009;360(6):588–598.
4. Nair H, et al. Global burden of acute lower respiratory infections due to respiratory syncytial virus in young children: a systematic review and meta-analysis. *Lancet*. 2010;375(9725):1545–1555.
5. Fulginiti VA, Eller JJ, Sieber OF, Joyner JW, Minamitani M, Meiklejohn G. Respiratory virus immunization. I. A field trial of two inactivated respiratory virus vaccines; an aqueous trivalent parainfluenza virus vaccine and an alum-precipitated respiratory syncytial virus vaccine. *Am J Epidemiol*. 1969;89(4):435–448.
6. Kapikian AZ, Mitchell RH, Chanock RM, Shvedoff RA, Stewart CE. An epidemiologic study of altered clinical reactivity to respiratory syncytial (RS) virus infection in children previously vaccinated with an inactivated RS virus vaccine. *Am J Epidemiol*. 1969;89(4):405–421.
7. Kim HW, et al. Respiratory syncytial virus disease in infants despite prior administration of antigenic inactivated vaccine. *Am J Epidemiol*. 1969;89(4):422–434.
8. Cherukuri A, et al. An adjuvanted respiratory syncytial virus fusion protein induces protection in aged balb/c mice. *Immun Ageing*. 2012;9(1):21.
9. Smith G, et al. Respiratory syncytial virus fusion glycoprotein expressed in insect cells form protein nanoparticles that induce protective immunity in cotton rats. *PLoS One*. 2012;7(11):e50852.
10. McLellan JS, et al. Structure-based design of a fusion glycoprotein vaccine for respiratory syncytial virus. *Science*. 2013;342(6158):592–598.
11. Beeler JA, van Wyke Coelingh K. Neutralization epitopes of the F glycoprotein of respiratory syncytial virus: effect of mutation upon fusion function. *J Virol*. 1989;63(7):2941–2950.
12. Impact-RSV Study Group. Palivizumab, a humanized respiratory syncytial virus monoclonal antibody, reduces hospitalization from respiratory syncytial virus infection in high-risk infants. *Pediatrics*. 1998;102(3):531–537.
13. Meissner HC, Bocchini JA. Reducing RSV hospitalizations aap modifies recommendations for use of palivizumab in high-risk infants, young children. *AAP News*. 2009;30(7):1–1.
14. Wu H, Pfarr DS, Losonsky GA, Kiener PA. Immunoprophylaxis of RSV infection: advancing from RSV-IGIV to palivizumab and motavizumab. *Curr Top Microbiol Immunol*. 2008;317:103–123.
15. Arbiza J, et al. Characterization of two antigenic sites recognized by neutralizing monoclonal antibodies directed against the fusion glycoprotein of human respiratory syncytial virus. *J Gen Virol*. 1992;73(pt 9):2225–2234.
16. López JA, et al. Antigenic structure of human respiratory syncytial virus fusion glycoprotein. *J Virol*. 1998;72(8):6922–6928.
17. McLellan JS, Chen M, Kim A, Yang Y, Graham BS, Kwong PD. Structural basis of respiratory syncytial virus neutralization by motavizumab. *Nat Struct Mol Biol*. 2010;17(2):248–250.
18. Wu H, et al. Development of motavizumab, an ultra-potent antibody for the prevention of respiratory syncytial virus infection in the upper and lower respiratory tract. *J Mol Biol*. 2007;368(3):652–665.
19. Toiron C, López JA, Rivas G, Andreu D, Melero JA, Bruix M. Conformational studies of a short linear peptide corresponding to a major conserved neutralizing epitope of human respiratory syncytial virus fusion glycoprotein. *Biopolymers*. 1996;39(4):537–548.
20. López JA, Andreu D, Carreño C, Whyte P, Taylor G, Melero JA. Conformational constraints of conserved neutralizing epitopes from a major antigenic area of human respiratory syncytial virus fusion glycoprotein. *J Gen Virol*. 1993;74(pt 12):2567–2577.
21. McLellan JS, et al. Design and characterization of epitope-scaffold immunogens that present the motavizumab epitope from respiratory syncytial virus. *J Mol Biol*. 2011;409(5):853–866.
22. Murata Y, Lightfoote PM, Rose RC, Walsh EE. Antigenic presentation of heterologous epitopes engineered into the outer surface-exposed helix 4 loop region of human papillomavirus l1 capsomeres. *Virol J*. 2009;6:81.
23. Correia BE, et al. Proof of principle for epitope-focused vaccine design. *Nature*. 2014;507(7491):201–206.
24. Bachmann MF, Jennings GT. Vaccine delivery: a matter of size, geometry, kinetics and molecular patterns. *Nat Rev Immunol*. 2010;10(11):787–796.
25. Milich DR, Chen M, Schödel F, Peterson DL, Jones JE, Hughes JL. Role of B cells in antigen presentation of the hepatitis B core. *Proc Natl Acad Sci U S A*. 1997;94(26):14648–14653.
26. Lee BO, et al. Interaction of the hepatitis B core antigen and the innate immune system. *J Immunol*. 2009;182(11):6670–6681.
27. Conway JF, et al. Hepatitis B virus capsid: localization of the putative immunodominant loop (residues 78 to 83) on the capsid surface, and implications for the distinction between c and e-antigens. *J Mol Biol*. 1998;279(5):1111–1121.
28. Conway JF, Cheng N, Zlotnick A, Wingfield PT, Stahl SJ, Steven AC. Visualization of a 4-helix bundle in the hepatitis B virus capsid by cryo-electron microscopy. *Nature*. 1997;386(6620):91–94.
29. Whitacre DC, Lee BO, Milich DR. Use of hepadnavirus core proteins as vaccine platforms. *Expert Rev Vaccines*. 2009;8(11):1565–1573.
30. Wynne SA, Crowther RA, Leslie AG. The crystal structure of the human hepatitis B virus capsid. *Mol Cell*. 1999;3(6):771–780.
31. Billaud J, et al. Advantages to the use of rodent hepadnavirus core proteins as vaccine platforms. *Vaccine*. 2007;25(9):1593–1606.
32. Billaud J, et al. Combinatorial approach to hepadnavirus-like particle vaccine design. *J Virol*. 2005;79(21):13656–13666.
33. Walsh EE, Falsey AR. Age related differences in humoral immune response to respiratory syncytial virus infection in adults. *J Med Virol*. 2004;73(2):295–299.
34. Graham BS. Biological challenges and technological opportunities for respiratory syncytial virus vaccine development. *Immunol Rev*. 2011;239(1):149–166.
35. Delgado MF, et al. Lack of antibody affinity maturation due to poor toll-like receptor stimulation leads to enhanced respiratory syncytial virus disease. *Nat Med*. 2009;15(1):34–41.
36. Milich DR, Schödel F, Hughes JL, Jones JE, Peterson DL. The hepatitis B virus core and e antigens elicit different TH cell subsets: antigen structure can affect TH cell phenotype. *J Virol*. 1997;71(3):2192–2201.
37. Eschli B, et al. Early antibodies specific for the neutralizing epitope on the receptor binding subunit of the lymphocytic choriomeningitis virus glycoprotein fail to neutralize the virus. *J Virol*. 2007;81(21):11650–11657.
38. McLellan JS, et al. Structure of RSV fusion glycoprotein trimer bound to a prefusion-specific neutralizing antibody. *Science*. 2013;340(6136):1113–1117.
39. Coler RN, et al. Development and characterization of synthetic glucopyranosyl lipid adjuvant system as a vaccine adjuvant. *PLoS One*. 2011;6(1):e16333.